atmosphere

MDPI

Article

Health Risk Appraisal Associated with Air Quality over Coal-Fired Thermal Power Plants and Coalmine Complex Belts of Urban–Rural Agglomeration in the Eastern Coastal State of Odisha, India

Arti Choudhary [1,2,*], Pradeep Kumar [3], Saroj Kumar Sahu [2], Chinmay Pradhan [2], Pawan Kumar Joshi [3,4], Sudhir Kumar Singh [5], Pankaj Kumar [6,*], Cyrille A. Mezoue [7], Abhay Kumar Singh [8] and Bhishma Tyagi [9]

1 Center for Environment, Climate Change and Public Health, Utkal University, Bhubaneswar 751004, India
2 Department of Botany, Utkal University, Bhubaneswar 751004, India
3 School of Environmental Sciences, Jawaharlal Nehru University, New Delhi 110067, India
4 Special Centre for Disaster Research, Jawaharlal Nehru University, New Delhi 110067, India
5 K. Banerjee Centre of Atmospheric and Ocean Studies (KBCAOS), IIDS, Nehru Science Centre, University of Allahabad, Prayagraj 211002, India
6 Adaptation and Water Department, Institute for Global Environmental Strategies, Hayama 240-0115, Japan
7 National Higher Polytechnic School Douala, University of Douala, Douala P.O. Box 2701, Cameroon
8 Department of Physics, Institute of Science, Banaras Hindu University, Varanasi 221005, India
9 Department of Earth and Atmospheric Sciences, National Institute of Technology, Rourkela 769008, India
* Correspondence: choudharyarti12@gmail.com (A.C.); kumar@iges.or.jp (P.K.)

Abstract: Manufacturing and mining sectors are serious pollution sources and risk factors that threaten air quality and human health. We analyzed pollutants at two study sites (Talcher and Brajrajnagar) in Odisha, an area exposed to industrial emissions, in the pre-COVID-19 year (2019) and consecutive pandemic years, including lockdowns (2020 and 2021). We observed that the annual data for pollutant concentration increased at Talcher: $PM_{2.5}$ (7–10%), CO (29–35%), NO_2 and NO_x (8–57% at Talcher and 14–19% at Brajrajnagar); while there was slight to substantial increase in PM_{10} (up to 11%) and a significant increase in O_3 (41–88%) at both sites. At Brajrajnagar, there was a decrease in $PM_{2.5}$ (up to 15%) and CO (around half of pre-lockdown), and a decrease in SO_2 concentration was observed (30–86%) at both sites. Substantial premature mortality was recorded, which can be attributed to $PM_{2.5}$ (16–26%), PM_{10} (31–43%), NO_2 (15–21%), SO_2 (4–7%), and O_3 (3–6%). This premature mortality caused an economic loss between 86–36 million USD to society. We found that although lockdown periods mitigated the losses, the balance of rest of the year was worse than in 2019. These findings are benchmarks to manage air quality over Asia's largest coalmine fields and similar landscapes.

Keywords: criteria pollutants; coal clusters; impact of pollutants; human health risk; premature mortality; economic cost

Citation: Choudhary, A.; Kumar, P.; Sahu, S.K.; Pradhan, C.; Joshi, P.K.; Singh, S.K.; Kumar, P.; Mezoue, C.A.; Singh, A.K.; Tyagi, B. Health Risk Appraisal Associated with Air Quality over Coal-Fired Thermal Power Plants and Coalmine Complex Belts of Urban–Rural Agglomeration in the Eastern Coastal State of Odisha, India. *Atmosphere* **2022**, *13*, 2064. https://doi.org/10.3390/atmos13122064

Academic Editors: Boris Igor Palella and Anil Namdeo

Received: 3 November 2022
Accepted: 5 December 2022
Published: 8 December 2022

1. Introduction

Air pollution is a global problem and measures to fix it need to be identified [1]. Growth in population, urbanization, industrialization, motorization, and modernization has increased the pace of air pollution and has pushed it beyond a self-repairable limit [2]. The effects of air pollutants and their synergistic interactions are known to affect multiple resources, including life forms, biodiversity, heritage and property of national interest, and human well-being and life [2,3]. According to the World Health Organization (WHO) database on global air pollution, 14 out of 15 cities having the worst air pollution are in India [4]. The primary anthropogenic emission sources of particulate matter ($PM_{2.5}$ and PM_{10}) are households, industries, and transport sectors [5–7]. Among gaseous pollutants, oxides

of nitrogen (NO_x) and sulphur dioxide (SO_2) emissions are dominated by transport [8], industry, and coal-based thermal power plants [9]; carbon monoxide (CO) emissions are the result of incomplete combustion of fuels used in residential biomass burning, the transport sector, and industry [10]. SO_2, nitrogen dioxide (NO_2), and PM are common, but more profoundly available in industrial and urban landscapes [11].

Several epidemiological studies have reported increased morbidity and mortality due to PM exposure [12]. Globally, an average increase in mortality per 10 mg/m^3 changes in ambient PM concentrations at all low and high estimates were reported as 0.34% and 0.75%, respectively [13], whereas a combined analysis for four cities in Asia was estimated by the Public Health and Air Pollution in Asia (PAPA) program to have an average of 0.55% increase in mortality per 10 mg/m^3 change in ambient PM_{10} concentrations [14]. Most of the earlier studies described acute effects from exposure to PM_{10}, SO_2, and NO_2, whereas the recent studies focused on the acute effects of exposure to $PM_{2.5}$, ozone (O_3), and CO. A meta-analysis in China demonstrated that exposure to PM_{10}, $PM_{2.5}$, SO_2, NO_2, O_3, and CO is significantly associated with increased all-cause and cardio-respiratory mortality risks [15].

The widespread and rapid social and economic changes in response to COVID-19 were expected to bring improvements in air quality at large and for hotspots in particular. Scholars have reported significant improvement in air quality due to COVID-19 shutdowns in 2020 [16]. In 330 Chinese cities and New York (USA), air quality improved by 11% and 50%, respectively [17]. As reported in many towns and cities across India, around 20–60% reduction in $PM_{2.5}$, PM_{10}, SO_2, and NO_2 and 10–60% increase in daytime O_3 concentrations were witnessed due to lockdowns [17]. During COVID-19 lockdowns, significant reductions in pollutants were also observed over the megacities of India [18,19]. These reductions in air pollution provide an opportunity to re-draw maps of natural and reduced emissions in order to understand the baseline air pollution over different regions.

Industrial and mining sector development is the engine of economic growth in developing nations. In India, the eastern coastal state of Odisha is known for intensive manufacturing and mining. Talcher is a town in the Angul district and Brajrajnagar is a town in the Jharsuguda district, the industrial areas of the state. The Angul–Talcher industrial area has been identified as one of the world's largest emissions hotspots [20]. With the increasing mechanization of mines, more fine dusts hazardous to human health were generated [21]. Cropper et al. [22] reported that coal field sites areas' average damage per ton are greater for directly emitted $PM_{2.5}$ (23 deaths per 1000 t of $PM_{2.5}$) than for SO_2 (10 deaths per 1000 t of SO_2) or NO_x (9 deaths per 1000 t of NO_x). In 2017, Talcher was identified as one of the critically polluted industrial areas in the CPCB report 'Comprehensive Environmental Pollution Index (CEPI)' [23]. A plethora of research articles reported and represented the impact of lockdowns on air quality in several aspects [16–19]. However, there are few scientific reports that consider coal-fired thermal power plants and coal-mining clusters [22] to elucidate the air quality during lockdown and pandemic years [23]. Accordingly, we analyzed the air quality of two towns recognized as constituting the hub of thermal power plants and coalmine clusters. The objectives of this study were to estimate (i) the trends in air pollutants parallel to mortality and economic loss, and (ii) to perform a health risk analysis in the eastern coastal state Odisha, India. Our analysis will be important and represent the area as well as the intense mining, manufacture, and industrial sectors, and will enable public health authorities and policymakers to take the necessary preventative actions to combat air pollution.

2. Research Design

2.1. Study Area

The Talcher coalmine belts and Brajrajnagar open-cast mines are identified as the major hotspot of poor air quality in Odisha, India [23]. Talcher (site #1, 20.95° N, 85.23° E), a town in the Angul district, is well known for coal mines and huge deposits of coal. The area is situated on the right bank of the Brahmani River and is one of the fastest-growing

industrial and mining complexes in the country. The climate is tropical, with summers having higher rainfall (330.20 mm) than the winters (12.70 mm). The average annual temperature is 26.8 °C. A large portion of the district is covered by forests (42.16%), with a variety of minor and major forest produce [24]. There are 11 coal mines covering 10,474.3 ha, 1 sand (stow) mine (17.5 ha), and 1 quartz mine (10.7 ha) [25]. The large industrial clusters include the Mahanadi Coal Field Ltd. (MCL), Odisha, India, the Talcher Thermal Power Station (TTPS), Odisha, India and the National Aluminum Company Ltd. (NALCO) plant, Bhubaneswar, India. In addition, coal-based thermal power plants, heavy industries, coal washeries, and subsidiary industrial units are situated in the area [23].

Brajrajnagar (site #2) is a city and municipality in the Jharsuguda district known for its coal mines. It has numerous open-cast and underground coal mines in the locality of the Ib valley coalfield region [26]. The town is small, located on rocky terrain on the banks of the Ib River (21.82° N, 83.92° E). The CPCB [27] reported that 78% of the cities in the Air Quality Index (AQI) bulletin fall into the good and satisfactory categories, and the remaining 12% of cities still had poor air quality during the lockdown phase, although only 44% cities had good air quality in the pre-lockdown phase. The geo-locations of the study area are presented in Figure 1 (Supplementary Table S1).

Figure 1. Map of study area map.

2.2. Data Resources

Air quality data were extracted for the period of 1 January 2019 to 31 May 2021 from the CPCB stations installed at Talcher and Brajrajnagar. We analyzed the spatiotemporal variation in criteria pollutants from 2019 to 2021 and the COVID-19 interventions phase between 25 March–31 May 2020 and 5 May–31 May 2021. For comparative analysis of a whole year, 2019 was taken as the base year in order to understand the comprehensive distribution of air pollutants at site #1 and site #2. The seven criteria pollutants ($PM_{2.5}$, PM_{10}, NO_x, NO_2, SO_2, O_3, and CO) were analyzed over the sites. The quality of data was ensured by filtering zeroes, negative values, erroneous data, and outliers. The greatest amount of

missing data was observed for NO_2 and NO_x at site #2 and SO_2 at both of the sites. The hourly pollutant data were collected for the diurnal variation, while data were converted to 24 h averages for time series analysis. The daily averaged meteorological parameters, namely relative humidity (RH), temperature (°C), wind speed (WS), and precipitation (PCPN) at a spatial resolution of 0.5° × 0.5° (MERRA-2 model) were collected from the NASA (National Aeronautics and Space Administration, Washington, DC, USA) POWER website. Population and death rates for three years (2019–2021) were estimated using census data for the year 2011. The health risk analysis was performed using epidemiological equations. The datasets were filtered in order to have a more consistent time series. Both sites had around 75% of valid data points that were used in analysis.

2.3. Health Risk, Mortality, and Economic Loss

We analyzed the health risks associated with the criteria pollutants (PM_{10}, $PM_{2.5}$, NO_2, SO_2, CO and O_3). The mortality or health endpoint is taken into account for health risk evaluation studies, since death is the most clearly defined health endpoint. It assumes that all incidences are the result of the exposure concentration in any area (Table S2). We determined the relative risk (*RRi*) for each pollutant, estimated based on health effect studies (Equation (1)); the excess risk (*ER*) (Equation (2)); and the attribution factor (AF_i) to estimate the impact of exposure variations (Equation (3)) [28]:

$$RR_i = \exp[\beta_i \times (C_i - C_{i,0})],\ C_i > 0 \quad (1)$$

$$ER_i = RR_i - 1 \quad (2)$$

$$AF_i = (RR_i - 1)/RR_i \quad (3)$$

where β_i was the exposure–response relationship coefficient, representing the *ER* of a health effect (such as mortality) per unit increase of pollutant (i.e., 1 μg/m^3 of $PM_{2.5}$); C_i is the absolute concentration of pollutant *i*, and C_0 is the threshold concentration below which a pollutant demonstrates no obvious adverse health effects (i.e., RR_i = 1). C_0 was considered 0 for all pollutants except CO, whose threshold value was taken as 4 mg/m^3. Therefore, air pollutants exert *ER* of mortality only when they are above the given thresholds, that is, RR_i−1. For this study, β values were chosen from daily mortality for all ages: 0.38% ($PM_{2.5}$), 0.32% (PM_{10}), 0.81% (SO_2), 1.30% (NO_2), and 0.48% (O_3) per 10 μg/m^3, and the β value was 3.7% per 1 mg/m^3 increase in CO [28]. The premature deaths (*PD*) due to different criteria pollutant exposure was calculated using Equation (4):

$$PD_i = n_i \times AF_i \quad (4)$$

where PD_i is the premature death from pollutant *i*; n_i is the total number of deaths due to pollutant *i*; and AF_i is the attribution factor of pollutant *i*.

Due to the unavailability of a market value for human lives, the monetary burden due to health risks was calculated using the value of statistical life (VSL) method. We estimated that $PM_{2.5}$, PM_{10}, NO_2, SO_2, and O_3 were responsible for economic costs in Talcher and Brajrajnagar due to the reported health endpoints, using the following equation (Equation (5)):

$$EC_{mort} = n_i \times VSL_i \quad (5)$$

where EC_{mort} is the economic cost per year of $PM_{2.5}$-, PM_{10}-, NO_2-, SO_2-, and O_3-related premature mortality at site #1 and site #2 and n_i is the number of premature deaths due to particular pollutants. VSL_i is the Indian value of statistical life. The OECD (Organization for Economic Cooperation and Development, 2014) gave an Indian VSL_i value of 0.60 million USD for 2010, while [29] reported 1.10 million USD for 2011. Shanmugam [30] carried out a VSL study in India during the year 1996–1997 and the value ranged from 0.17–0.23 million USD. Furthermore, Cropper et al. [31] estimated a VSL for India in the

range of 0.08–0.18 million USD. In the current study, we used the most recent value of VSL, i.e., 0.59 million USD estimated in the year 2016 [32].

3. Results

3.1. Spatiotemporal Variation of Air Pollutants

We found positive and negative fluctuations in air pollutants in two consecutive pandemic years as well as during two lockdown periods at both sites in comparison to the base year 2019 (the average absolute values are reported in Table 1). The two successive phases of lockdown can be assumed as two sets of experiments that represent conditions in the absence of human activities (i.e., the forced shutdown offers zero background concentration). The diurnal temporal variation and pollutant correlation with meteorology are reported in detail in Sections 3.1–3.3 (Table S3).

Table 1. Average concentration and standard deviation of pollutants during two successive lockdowns (25 March–31 May 2020 and 5 May–31 May 2021) and the base year (period from 25 March–31 May 2019).

Year	$PM_{2.5}$	PM_{10}	CO	SO_2	NO_2	NO_x	O_3
	($\mu g/m^3$)		(ppm)	(ppb)			
				Site #1			
2019	38.80 ± 13.54	159.36 ± 53.28	1.23 ± 0.29	25.98 ± 2.96	13.06 ± 3.48	25.33 ± 4.49	5.41 ± 1.83
LD2020	41.66 ± 22.11	165.15 ± 92.33	1.88 ± 0.31	19.88 ± 6.69	12.76 ± 9.45	24.94 ± 18.68	44.87 ± 9.29
LD2021	37.92 ± 10.12	162.14 ± 55.89	1.73 ± 0.27	13.84 ± 4.96	28.22 ± 5.78	49.00 ± 7.78	25.33 ± 5.04
				Site #2			
2019	69.88 ± 31.51	152.88 ± 54.76	2.65 ± 0.50	7.51 ± 1.26	19.66 ± 4.25	29.85 ± 9.56	10.96 ± 3.61
LD2020	78.35 ± 30.61	171.94 ± 64.57	1.11 ± 0.28	4.92 ± 1.05	3.35 ± 1.64	20.42 ± 5.10	54.91 ± 15.08
LD2021	61.09 ± 11.56	143.29 ± 28.32	2.26 ± 0.13	4.83 ± 0.49	22.02 ± 10.07	37.55 ± 9.66	21.79 ± 16.69

3.1.1. Particulate Matter

The analysis of pandemic years 2020 and 2021 revealed that the average concentration of $PM_{2.5}$ marginally varied between 2–10 $\mu g/m^3$ in 2020–2021, but the daily fluctuations were equal to or even higher than the pre-lockdown year (2019) at both sites. The spatiotemporal variation of $PM_{2.5}$ had a 7.1–10.3% increase during LD2020 and a 2.6–14.7% decrease during LD2021. Comparatively, moderate to higher continuous precipitation during LD2021 led to washout of pollutants. The drop in $PM_{2.5}$ concentrations was not noteworthy when compared to other cities (such as Delhi, Chennai, Kolkata, Bangalore, Hyderabad, and Mumbai, etc.), particularly during LD2020. This is important as site #1 and site #2 have numerous open-cast and underground coal mines and four units of thermal power plants that were operational during the LD period. The PM_{10} distribution showed similar trends to $PM_{2.5}$. PM_{10} concentrations varied between 1.8–11.0% during LD2020 and LD2021 at both sites compared to 2019 (Figures 2 and 3 and Table 1). Scholars have reported that surface- and satellite-based data both showed a 42–60% and 24–62% reduction in $PM_{2.5}$ and PM_{10}, respectively, in Indian megacities during LD2020 [33]. Other cities in Odisha also reported a significant drop in particulate matter concentration, except Talcher and Brajrajnagar. For example, in the capital city Bhubaneswar, a 10–42% drop in surface-based concentrations of $PM_{2.5}$ [34] and 33% in PM_{10} was reported during LD2020 as compared to the base year. Contrary to thermal power plant cities, semi- and moderately industrialized regions of India also reported a significant reduction in $PM_{2.5}$ and PM_{10} concentrations during LD2020. Thomas et al. [35] reported that concentrations of $PM_{2.5}$ (24–47%) and PM_{10} (17–20%) decreased, and the overall air quality of a less-industrialized region, Kerala (a southern coastal state of India), significantly improved. The PM_{10} concentration at the semi-industrialized town of Kannur, Kerala, declined by 61% [36].

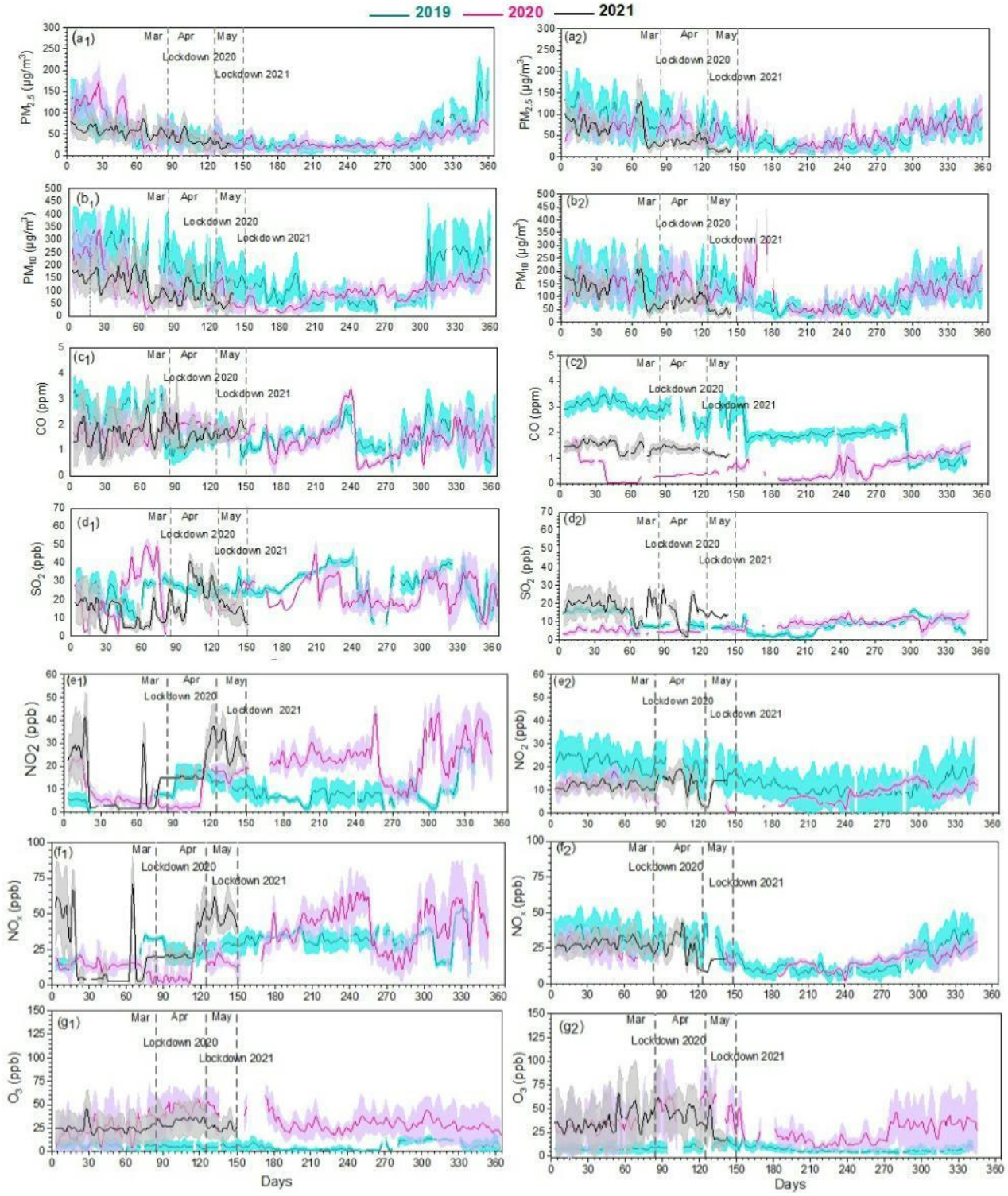

Figure 2. Trends in hourly averages of $PM_{2.5}$, PM_{10}, CO, SO_2, NO_2, NO_x, and O_3 concentrations between 2019–2021 (dotted 1st vertical line shows pre-LD period; 1st and 2nd vertical dotted line section shows LD2020; and 2nd and 3rd line section shows LD2021) for site #1 (**a1**–**g1**) and site #2 (**a2**–**g2**).

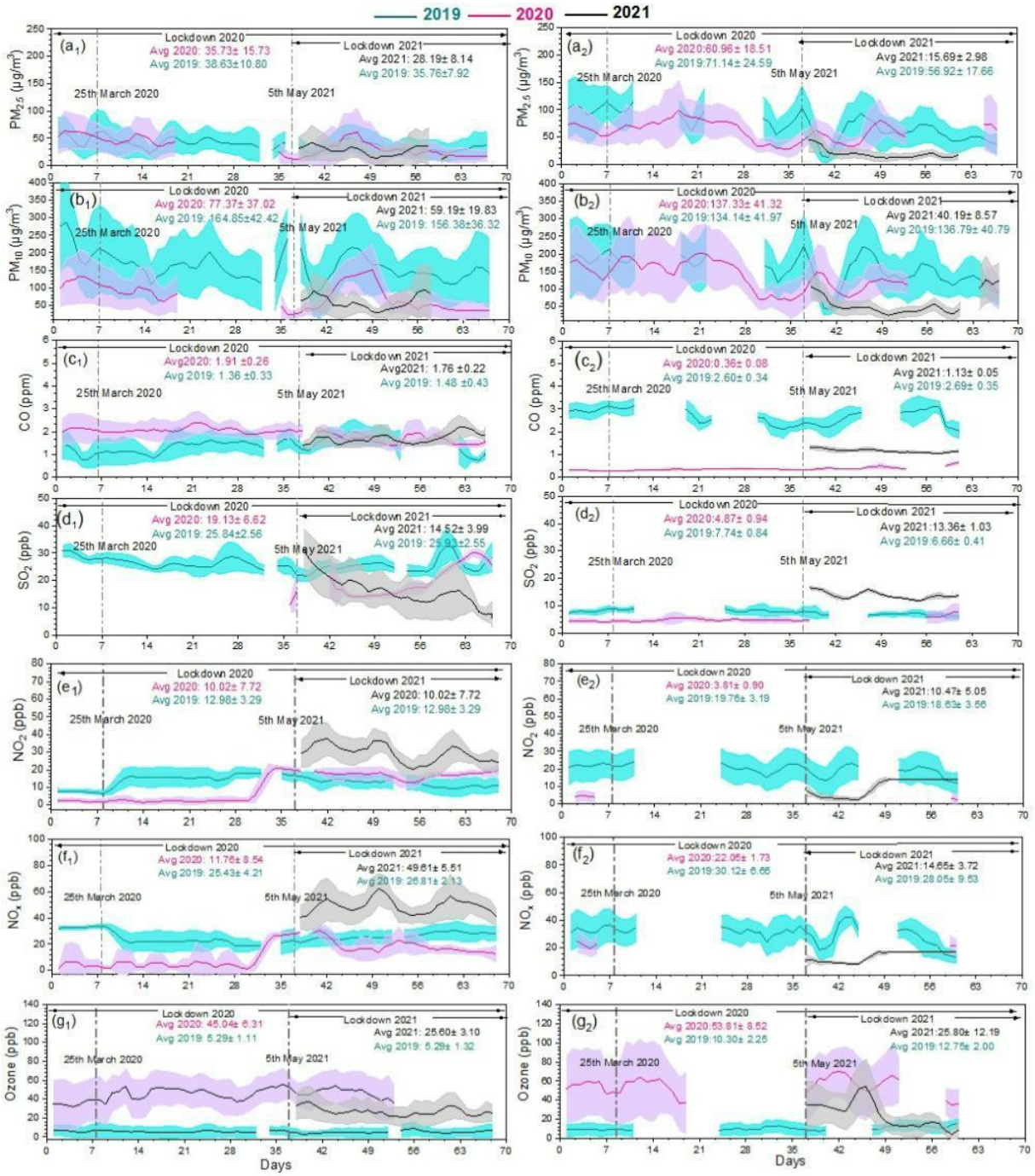

Figure 3. Temporal variation in pollutants $PM_{2.5}$, PM_{10}, CO, SO_2, NO_2, NO_x, and O_3 during LD2020 and LD2021 at site #1 ($\mathbf{a_1}$–$\mathbf{g_1}$) and site #2 ($\mathbf{a_2}$–$\mathbf{g_2}$) (dotted vertical line shows the start of LD2020 and LD2021).

3.1.2. CO

We found fluctuations in CO concentration at site #1 (Figures 2 and 3) during LD2020 and LD2021 compared to the base year. A decrease in CO concentrations at site #2 was especially observed during LD2020 and LD2021 as compared to the base year. The difference in the behavior of the two sites is the attribute of local anthropogenic emissions (coal burning in homes and small-scale commercial businesses like street-food cooking, agricultural waste burning, and biofuel burning). At site #1, a 29–35% increase in concentration was found during both consecutive lockdowns. The higher concentration at site #1 was possibly due to the forest fires and agricultural burning that are predominant during this season (March–May, pre-monsoon) [37,38]. The reduction in CO at site #2 (around 50%) may be

attributed to a limitation of combustion activities in different sectors such as transport, industry, and residential.

3.1.3. SO_2

A significant daily fluctuation (both positive and negative) in SO_2 concentration was observed at both sites in 2020–2021 as compared to 2019 (Figures 2 and 3 and Table 1). The overall SO_2 at both sites was found to have decreased (30–86%) as compared to the base year, which indicates a reduction of coal burning in small-scale commercial businesses like street-food cooking and biofuel burning, since utilization of sulphur-containing fuel or other coal-combustion activities were sluggish during lockdown [39]. The primary source of SO_2 is the combustion of sulphur-containing fuels such as coal and diesel used in thermal power plants, industries, and transport [39]. India is one of the highest emitters of anthropogenic SO_2.

3.1.4. NO_2 and NO_X

At site #1, during 2020 and 2021 both NO_2 (7.69–57%) and NO_x (8–45%) emissions varied when compared to the base year (Table 1 and Figures 2 and 3). It was observed that during LD2020, a large amount of data for NO_2 and NO_x was missing for site #2; therefore, average concentration was not depicting a representative variation. During LD2021, a 14–19% increase in NO_2 and NO_x concentrations was found in comparison to the base year. The oscillating peak of NO_x was showing a very similar follow-up trend to NO_2 within both site #1 and site #2 during LD2021. Ghude et al. [40] reported that the industrial and thermal power plant regions in India are major sources of nitrogenous emissions. The annual variations depict that throughout the years 2020 and 2021, NO_2 and NO_x concentrations were higher as compared to 2019, and this difference was very pronounced at site #1 as compared to site #2 (Figure 2). Some very sharp and high emission peaks were also observed at site #1, indicating local anthropogenic activity burning coal in the home, agricultural waste burning, and biofuel burning [41]. The reported concentration of NO_2 over a less-industrialized region (Kerala) showed a reduction of 48%, and NO_x 53–90% [35].

3.1.5. O_3

The daily time series plot (Figures 2 and 3) depicts significantly higher concentrations during LD2020 and LD2021 as compared to the base year. The O_3 concentration showed a uniformly increasing trend throughout the year (an increase of around 41–88% in 2020 and 2021; Table 1) and during the lockdown period. O_3 is a secondary pollutant that is formed in the presence of sunlight and its precursors, viz., NO_x and volatile organic compounds (VOCs). The rising CO concentration in 2020 and 2021 also indicates significant biomass burning, which possibly contributed to higher O_3 formation during lockdown periods as compared to the base year. It has been previously reported that among all the regions of India, biomass burning associated with O_3 production was observed to be highest over central Indian states like Odisha [38,39].

3.2. Air Pollutants and Meteorological Parameters

At site #1, RH was in weak correlation with pollutants NO_2 (r = 0.25), $PM_{2.5}$ (r = −0.25) at p (≤0.01) and NO_x and PM_{10} ($p \leq 0.001$); temperature had correlation with $PM_{2.5}$ (r = −0.19) at p (≤0.05), and WS with $PM_{2.5}$ and PM_{10} ($p \leq 0.001$). PM_{10} and $PM_{2.5}$ had strong correlation (r = 0.82), as did NO_2 and NO_x (r = 0.60); RH had a positive correlation (r = 0.48), and O_3 and NO_2 and NO_x also had positive correlation at different levels of significance (Figure 4a). At site #2, temperature, PCPN, and RH had positive correlation (r = 0.40), as did PM_{10} and $PM_{2.5}$ (r =0.94), $PM_{2.5}$ had positive correlation with NO_2, NO_x, and PM_{10}, whereas CO had positive correlation with NO_2 (r = 0.67). WS had positive correlation with temperature and PCPN. O_3 had negative correlation with PCPN and RH and was also negatively correlated with temperature and WS at p (≤0.001). At site #2, air

pollutants had good correlation with meteorological parameters as compared to site #1 (Figure 4 and Table S4). The correlation matrix of pollutants and meteorology did not depict any common behavior between the two sites. However, site #2 had comparatively better meteorology correlation with pollutants. At site #1, WS played a significant role in the distribution dynamic of PM.

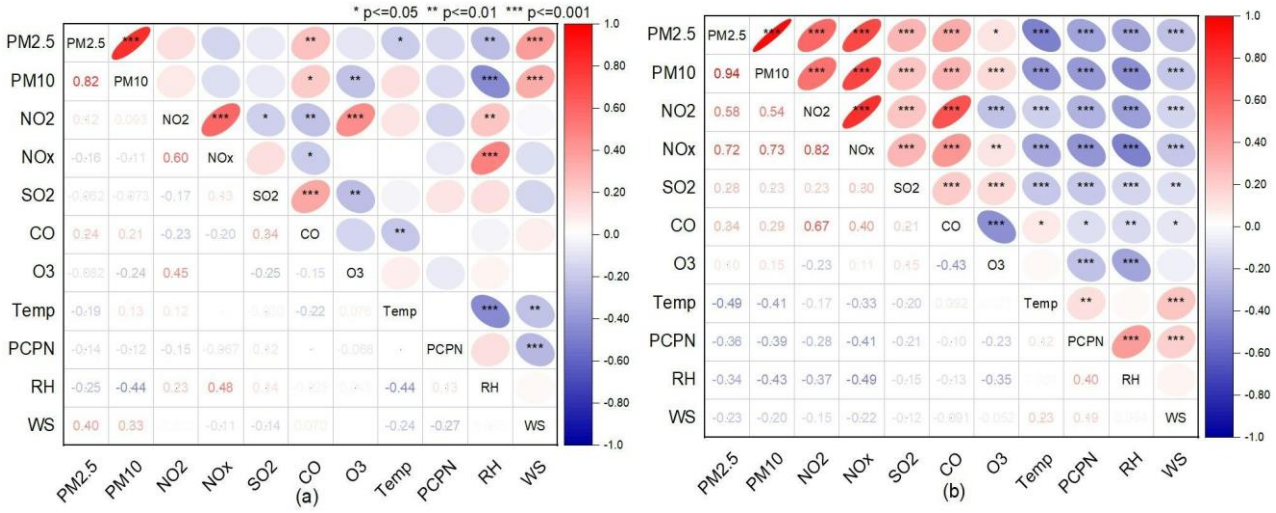

Figure 4. Correlation matrix of meteorological variables with pollutants at (**a**) site #1 and (**b**) site #2. (above diagonals: the more distorted the circle and darker the color, the closer the correlation was to 1; white: no correlation, blue: negative correlation, red: positive correlation; below diagonals: value of r, Pearson correlation coefficient; *: $p < 0.05$, **: $p < 0.01$; ***: $p < 0.001$).

3.3. Diurnal Variation of Pollutants

Diurnal variation of a pollutant was predominantly governed by local emissions, meteorological conditions, and daytime and nighttime chemistry. The diurnal variation of some criteria pollutants (O_3, NO_x, and NO_2) was found to be higher than the base year, whereas SO_2 concentrations were found to have decreased (Table S5a,b and Figure S1a–c). Some pollutants showed variation ($PM_{2.5}$, PM_{10}, and CO) across sites, which may be attributed to local meteorology and anthropogenic activities (coal burning in homes and small-scale commercial businesses like street-food cooking, agricultural waste burning, and biofuel burning).

3.3.1. Diurnal Variation of Particulate Matter

The diurnal variation of $PM_{2.5}$ and PM_{10} (Figure 5) followed a bimodal distribution. The first peak developed between 4 a.m. and 12 noon, and the second peak developed around 18 p.m. and 22 p.m. These peaks ranged from blunt ($PM_{2.5}$ and PM_{10} at site #1) to moderate ($PM_{2.5}$ and PM_{10} at site #2). We found both sites' PM concentration was more or less the same, particularly during LD2020 and compared to the base year. The diurnal trends also adhered to a daily variation pattern for particulate matter. During the LD2021 period, $PM_{2.5}$ and PM_{10} concentrations were found to be slightly lower than LD2020 and the base year concentration, especially from 4 a.m. to 12 noon and around 18 p.m. to 22 p.m. This drop in concentration may be due to reduced data points in LD2021 and washout of PM concentration. During 5−10 May 2021 there was heavy rainfall reported due to cyclone "Yaas" and frequent rains were observed throughout May 2021. The reduction in primary anthropogenic emissions may be the cause of variation in pollutant concentrations in different hours of the day. Mahato and Ghosh [42] reported a drastic drop (70%) in diurnal concentrations of PMs in LD2020.

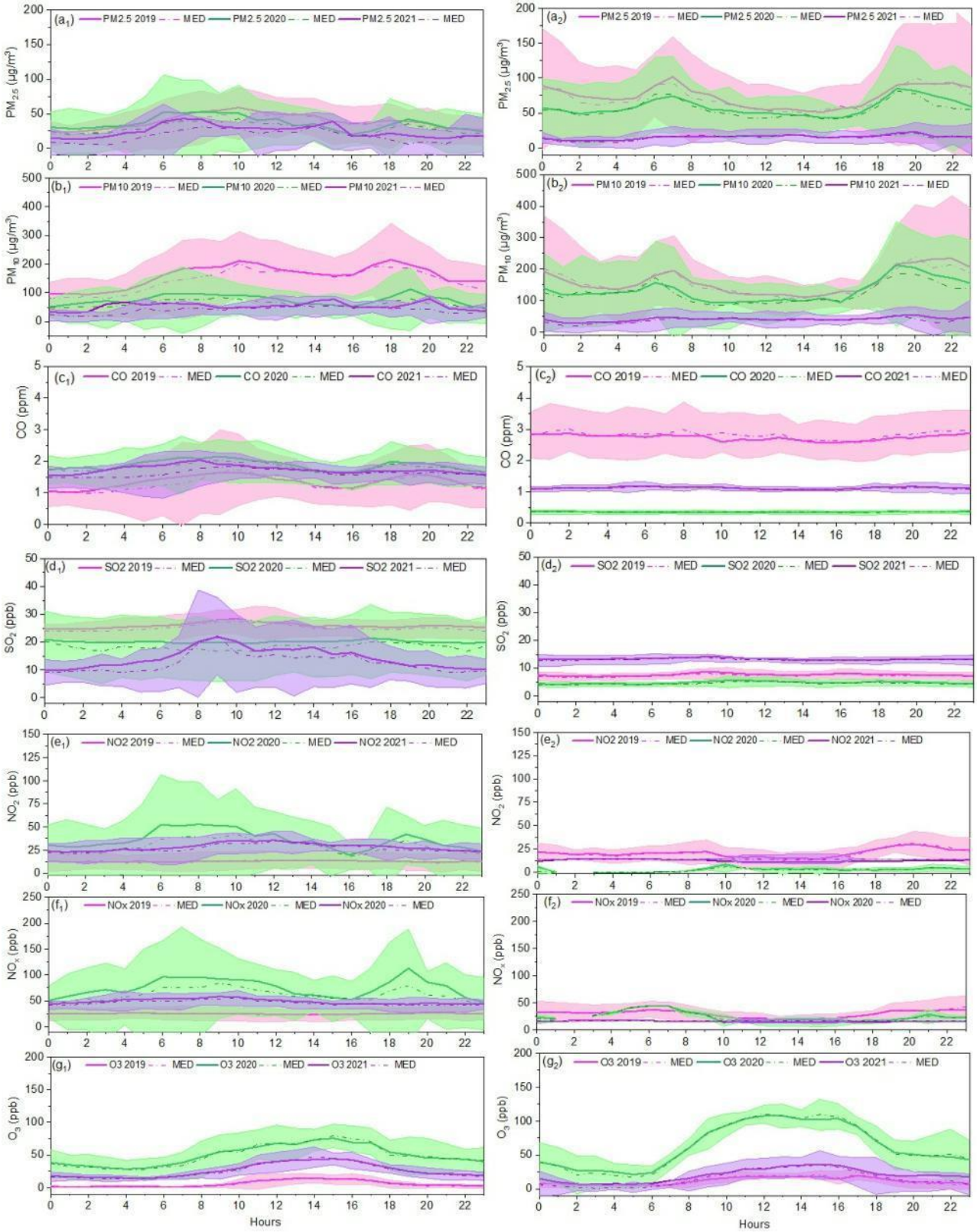

Figure 5. Average diurnal variation of $PM_{2.5}$, PM_{10}, CO, SO_2, NO_2, NO_x, and O_3 during LD2020, LD2021, and the coinciding base year 2019. Continuous and dotted lines represent mean and median, respectively, and the shaded region shows the IQR at site #1 (**a_1**–**g_1**) and site #2 (**a_2**–**g_2**).

3.3.2. Diurnal Variation of NO_2, NO_x, and O_3

The diurnal variation of NO_2 and NO_x showed an increasing concentration in the morning hours from 5 a.m. to 9 a.m., then in the proceeding hours it decreased, again increasing between 16 p.m. and 22 p.m. (Figure 5). This trend was clearly observed during LD2020 at site #1 for NO_2 and NO_x. At site #2, the NO_2 and NO_x concentration was found to be uniformly lower in the base year as compared to the LD2020 and LD2021. Due to missing data for NO_2 and NO_x at site #2 during LD2020, a representative trend could not be observed (Figure 5).

O_3 concentrations were found to be higher throughout day and night in LD2020 and LD2021 as compared to the pre-lockdown period of 2019. In LD2020, O_3 concentration was greatest, and clear emission peaks were observed between 8 a.m. and 8 p.m. at both sites. The LD2021 diurnal trend showed slight bulging peaks from 8 a.m. to 18 p.m., as in LD2020 (Figure 5). The diurnal O_3 variation profile shows similarity with the daily O_3 profile.

3.3.3. Diurnal Variation of CO

We observed that both sites had different diurnal trends for CO. At site #1 during LD2020 and LD2021, CO concentration remained higher compared to the base year (Figure 5), whereas at site #2 during LD2020 and LD2021, CO concentration remained lower as compared to the base year and LD2020 showed the lowest concentration. CO is a biomass- and traffic-related pollutant, owing to biomass activities [37] at site #1, whereas at site #2 lower concentration during the lockdown period was due to reduction in biomass burning as well as transport activity. The spatiotemporal and diurnal variability trend of CO suggests a diversity in sources.

3.3.4. Diurnal Variation of SO_2

SO_2 concentration was higher at both sites during the base year as compared to LD2020 and LD2021 (Figure 5). SO_2 concentration was observed to be greatest from 8 a.m. to 14 p.m. in 2019 at both sites. LD2021 showed a bulging peak from 8 a.m. to 14 p.m. at site #1 but the overall magnitude was low as observed in the daily and temporal variation profile. At site #2, no clear peak was observed. Diurnal variation indicated that there were some anthropogenic activities during LD2021 at both sites that involved coal burning. Unlike other urban regions in India, the diurnal variation of SO_2 over the eastern coastal state of Odisha showed elevated daytime values due to the predominant influence of regional emissions [43].

3.4. Comparative Fundamental Statistics of Pollutants

Overall, the $PM_{2.5}$ and PM_{10} for both sites showed a similar pattern of distribution. In the case of $PM_{2.5}$ most data were within the first and third quartile at both sites, except for LD2021 (Figure 6). In the case of NO_2 and NO_x pollutants, the distribution was entirely different for both sites. Site #1 violin plots depicted distinct fine bimodal distribution during LD2020 and skinnier and elevated outliers in the LD2021 violin. At site #1, higher concentrations during LD2020 and LD2021 were also observed as compared to the base year, and most observations were gathered around the first and third quartile ranges for NO_2 and NO_x. On the other hand, site #2 depicted very skinny violins with more outliers, particularly for LD2020, suggesting more missing data points. The SO_2 concentration was found to have decreased during LD2020 and LD2021 as compared the base year, and a smaller and skinnier violin shape indicates a deficiency of data points at both sites. Contrary to that of SO_2, O_3 concentration during LD2020 and LD2021 increased as compared to the base year; data were highly skewed with skinnier violins and more outliers (Figure 6). For LD2021, a skinnier shape is indicative of missing data points. The CO data distribution was found to be less skewed and showed higher probability of data around the first and third quartile. At site #1, CO showed a bimodal distribution and a rise in concentration during the lockdown period as compared to the base year. On the other hand, at site #2 more data were gathered around the mean, and the base year concentration was higher as

compared to the lockdown period. Overall, the LD2021 violins are very skinny and smaller in shape for all pollutants because of fewer data points—only 25 data points (5 May 2021 to 31 May 2021) as compared to the LD2020 and base year (68 data points).

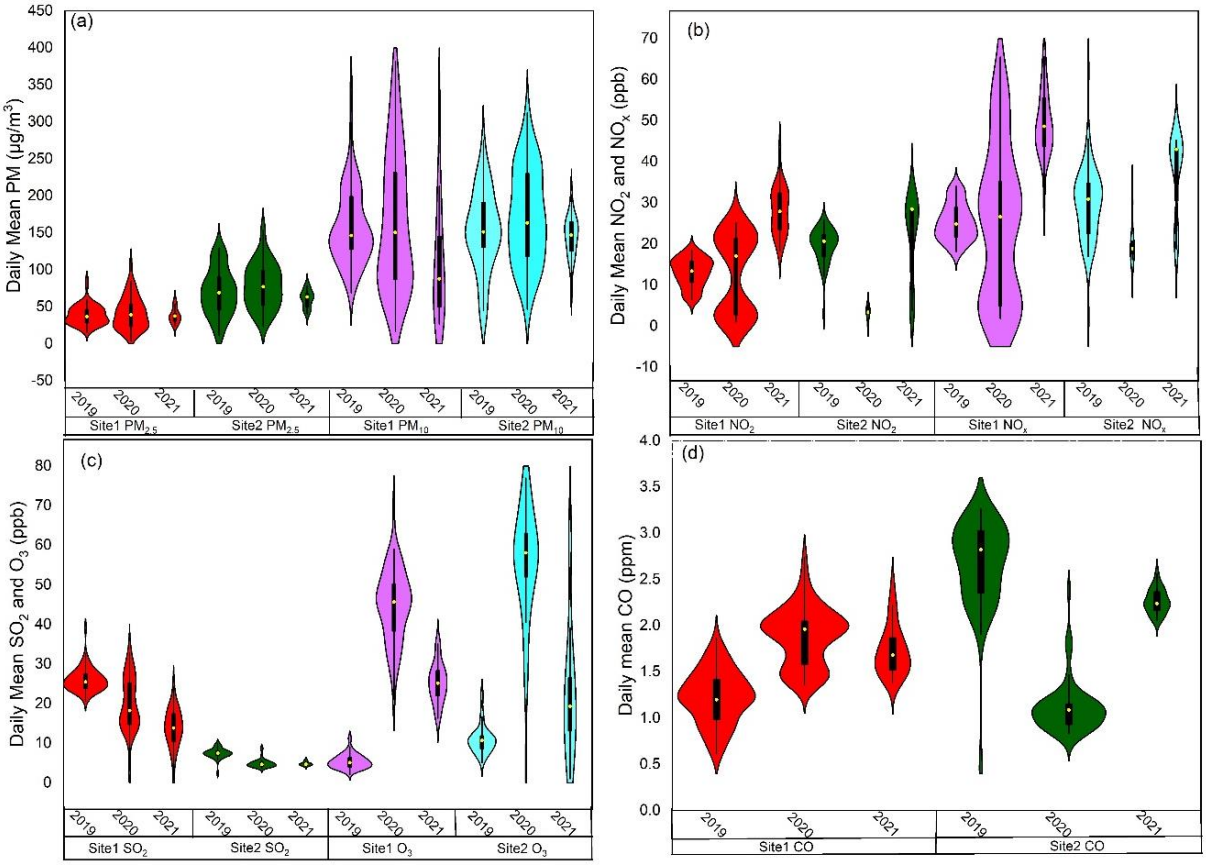

Figure 6. Violin plots of pollutant variations during LD2020, LD2021, and pre-lockdown year 2019 for site #1 and site #2 (thick black bar: interquartile range, central yellow dot: median, whiskers: $\pm 1.5 \times$ interquartile range). (**a**) Daily mean of PM, (**b**) Daily mean of NO_2 and NO_x, (**c**) Daily mean of SO_2 and O_3 and (**d**) Daily mean of CO.

4. Health Risk, Premature Death, and Economic Cost Associated with Pollutants

The health risk from air pollution in India is the focus of an international comparison. The study sites have an emission-intensive source of air pollution in their close environment (Table 2 and Figure 7). The CO concentration was found to be less than the minimum (CO = 2 mg/m^3) concentration; therefore, it was excluded from the health risk analysis in the present study. At both sites, the annual increase in total %ER ranged from 3−8% as compared to the base year. During LD, a 1-5% reduction in ER was found in 2020 and 2021. It can therefore be interpreted that the forced lockdown lowered the ER to 5% within the year, which was similar to the findings of [44]. Furthermore, at site #1 we found that atmospheric pollution caused 62−63% of annual deaths during the 2020−2021 period as compared to the base year. At site #2, atmospheric pollution caused 61−62% of total deaths annually in 2020 and 2021 as compared to 2019. We found that individually, particulate matters ($PM_{2.5}$: 16−26%; PM_{10}: 31−43%) and the gaseous pollutants O_3, SO_2, and NO_2 (O_3: 4−7%, SO_2: 11−25% and NO_2: 15−21%, Figure 7) were causing substantial premature mortality, similar to Cropper et al. [22].

Table 2. Details of excessive risk, premature death attribution, and economic cost at site #1 and site #2.

Sites	Year	Annual/ Lockdown	Pollutant-Wise Death Attribution/100,000					Total Attributed Deaths/100,000	EC (USD in Million)
			$PM_{2.5}$	PM_{10}	NO_2	SO_2	O_3		
Site #1	2019	Annual	47	84	26	24	6	187 (54%)	109
		Pre-lockdown	7	10	5	4	3	30 (52%)	17.6
	2020	annual	61	85	38	33	15	233 (63%)	137
		LD2020	7	11	9	6	4	37 (52%)	22
	2021	annual	62	113	32	17	8	232 (62%)	136
		LD2021	7	11	9	9	1	37 (60%)	22
Site #2	2019	annual	24	54	21	20	11	130 (58%)	76
		Pre-lockdown	5	10	2	2	0	19 (50%)	11
	2020	annual	31	56	27	25	8	147 (61%)	86
		LD2020	5	9	3	4	1	23 (58%)	14
	2021	annual	29	63	25	25	8	151 (62%)	89
		LD2021	5	10	4	4	1	24 (60%)	14

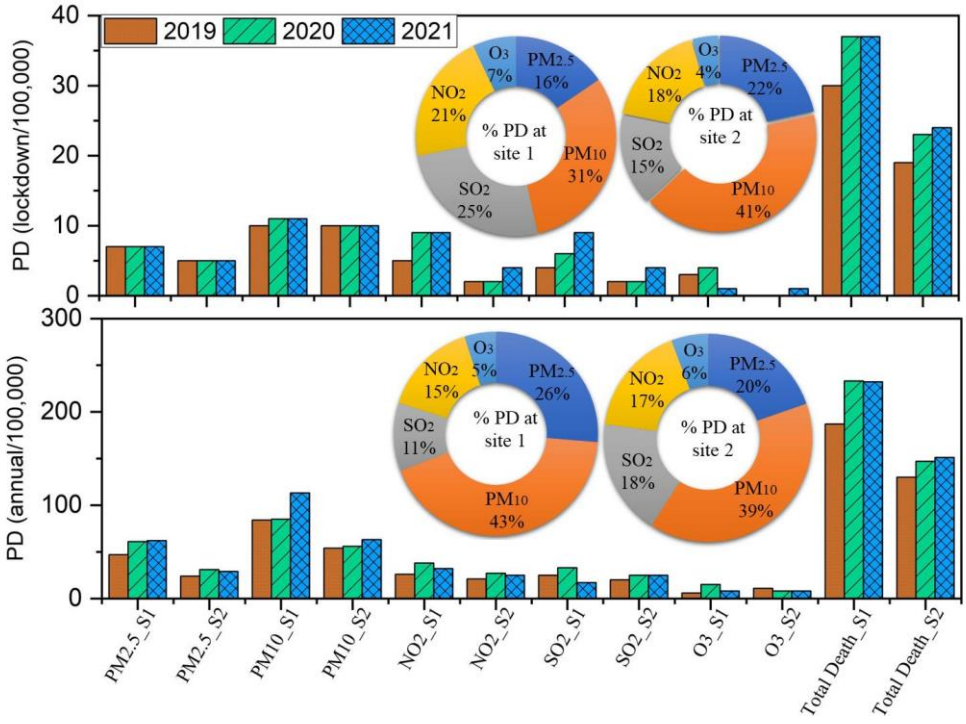

Figure 7. Pollutant-wise annual and lockdown period premature death (PD) attribution at site #1 and site #2.

Thermal power plant-having towns and cities always need extra care for their surrounding environment and at the same time need to attract the research community for local monitoring and analysis. Mishra (2015) [45] conducted 300 interviews in Angul−Talcher; five villages were 3.5 km or less from mines, and two were approximately 47 km away. From the villager interviews he concluded that 90% of households in the mining villages reported health problems, compared with 52% in non-mining villages in recent years. Another study reported that a quarter of the ambient $PM_{2.5}$ in southeastern coastal states like Tamil Nadu, Andhra Pradesh, and Odisha were coming from coal-fired power plants. This increased ambient $PM_{2.5}$ concentration from power plants led to 44% of deaths and attributable deaths. Our results were also close to previously reported results [46]. A forecast reported that Odisha's coal-based thermal power plants led to 6100 deaths in 2017 and 7560 deaths in 2020 [46]. Our results were also close to the previously reported results [45,47].

At site #1, the annual EC of total mortality due to air pollution was 109 million USD in 2019 and it increased to 137 million USD in 2020 and 136 million USD in 2021. At site #1, lockdown period air pollution mortality costs slightly increased to 22 million in 2020 and 2021 from 17.6 million in the pre-lockdown period of base year 2019. The annual EC of air pollution-attributed mortality at site #2 was 76 and 86 million USD in year 2019 and 2020, respectively, and it increased to 89 million USD in 2021. For the pre-lockdown period at site #2, we found that the EC was 11 million USD in 2019 and increased to 14 million USD in 2020 and 2021.

5. Discussion

The forced lockdown gave an opportunity for nature to sprout after hundreds of years and provided an opportunity for specialists and policymakers as well to conduct a close and comprehensive study of the effect of anthropogenic emissions during switch-off situations in various areas of the earth–atmosphere system. Contrary to cities with thermal power plants, semi- and moderately industrialized regions of India reported significant reduction in $PM_{2.5}$ and PM_{10} concentrations during LD2020 [35,36]. Most of the cities of Odisha also reported a significant drop in particulate matter concentrations [34] except Talcher and Brajrajnagar. We found trivial spatiotemporal deviation in $PM_{2.5}$ (7−10% increase at site #1 and up to a 15% drop at site #2) and a slight to substantial increase in PM_{10} (up to 11%) as compared to the base year. CO is a biomass- and traffic-related pollutant, attributable to biomass use [37] at site#1, though at site #2 lower concentrations during the lockdown timeframe were attributable to a decrease in biomass use as well as transport movement. The substantial drop in SO_2 (28% to 53%) demonstrated a decrease in nearby anthropogenic action [39], since use of sulphur-containing fuels or other coal-ignition sources was idle during 2020 and 2021 when contrasted with 2019. However, in the state capital city of Bhubaneswar, SO_2 was overwhelmed by provincial emissions as opposed to neighborhood sources [34,43]. O_3 was found to be higher over the course of LD2020 and LD2021 when contrasted with the pre-lockdown period of 2019. O_3 concentration is governed by several bio-geophysical elements [48–50]. We found a significant increase in O_3 (41–88%). The industrial and thermal power stations in India are significant wellsprings of nitrogenous discharges [40]. Some extremely sharp and high discharges were found at site #1, demonstrating neighborhood anthropogenic action [41]. The decrease in essential anthropogenic outflows might be a reason for the variability in nitrogenous oxide fixation in several hours of the day.

To comprehend the financial effect of the thermal power plant and coal-mine complex belt, we further assessed excessive health risk, pollutant-specific mortality attribution, probability of death, and associated economic loss. The effect of health risk, pollutant mortality attribution, probability of death, and economic loss are closely related. The coalmine complex belt and thermal power station-related uses were functional during 2020 and 2021, however everyday scheduled business was halted and both large- and limited-scope shops were shut, so it tends to be construed that the constrained lockdown brought ER down 5% in contrast to the base year. At an individual level, particulate matters ($PM_{2.5}$: 16−26%; PM_{10}: 31−43%) cause significantly higher mortality attribution than gaseous pollutants (4−25%), eventually causing substantial premature mortality. This led to a minor increase in societal cost of around 136 million USD in 2020 to 2021, which was 109 million USD in 2019. All the quantified results indicate that technical, economic, environmental, and social possibilities should be adopted in processing and mining coal for a possible sustainable solution [51].

6. Conclusions

We quantified variation in criteria pollutants at temporal scales (diurnal, daily, LD2020, and LD2021) and at a spatial scale (Talcher and Brajrajnagar sites). The coalmine complex clusters and coal-fired thermal power plants were continuously operational during the lockdown. Therefore, the findings elucidate the impact of thermal power plants and coalmine

complex sites on air quality in an eastern coastal state of India. The $PM_{2.5}$ increased by about 5−12% and PM_{10} by 3−13% during LD2020 and LD2021 at both sites. CO showed spatial variation at site #2, around a 17-54% drop, and at site #1, a 52−54% increase was observed, indicating the contribution of local activities such as forest fires, agricultural waste burning, and biofuel. Meanwhile, SO_2 and O_3 depicted contrasting trends to each other, with SO_2 illustrating a uniformly decreasing trend (28−53%) and O_3 portraying a uniformly increasing trend (41−88%) during both the pandemic year and lockdown periods. NO_2 and NO_x concentration presented random behavior, either vaguely increasing or remaining the same as the base year (8−57% temporal deviation at site #1 and 14−19% rise at site #2). The current study results conflict with other cities and industrial sites in India and around the world in reference to the pandemic year and COVID-19 lockdowns.

These pollution sources pose a significant health risk, as well as mortality and economic loss at a regional and state level. The results suggest that irrespective of pandemic restrictions excessive risk increased 3−8% and premature death increased 58−62% compared to the base year 2019. Except for CO and O_3, all criteria pollutants caused substantial attribution of premature mortality ($PM_{2.5}$: 16−26%; PM_{10}: 31−43%; NO_2: 15−21% and SO_2: 4−7%). This cost society 86−136 million USD. The results also advocate the need for improved emission regulations in coal clusters and coal-based thermal power plants. The results are significant as well as indicative that in order to clean the environment we should shift toward green energy sources for power and energy production. In parallel, governments must take the pollution issue seriously in these coal clusters and industrial belts, and environmental standards must be enforced and strictly maintained. The results demonstrate the need for replacement of fossil fuels by renewable energy sources, and the results should put pressure on local bodies toward meeting 2030 carbon emission reduction targets in India. The results may be handy for decision makers and local engineers for environmental management and for new insights in terms of air quality modelling, since several models are now used, as a real-world tool for improved and efficient management of the environment.

Supplementary Materials: The following supporting information can be downloaded at: https://www.mdpi.com/article/10.3390/atmos13122064/s1, Table S1: Potential sources of air pollution in the study area; Table S2: Descriptive statistics for meteorological parameters and air pollutants; Table S3: Meteorological parameters (wind speed, temperature, precipitation (PCPN) and relative humidity (RH) of studyareas during lockdown period (25 March–11 May); Table S4: The primary basic details of health risk analysis at site #1 and site #2; Table S5: Percentage change in the concentration of pollutant during the two succeeding lock-down; Table S6: (a) Hourly absolute difference and percentage change in pollutant concentration for site#1. (b) Hourly absolute difference and percentage change in pollutant concentration for site#2; Figure S1: (a) Average diurnal variation of $PM_{2.5}$ and PM_{10} during LD2020 and LD2021 and co-inciding base year 2019. Continuous line and the dotted line represent the mean and median re-spectively at site #1 and site #2. (b) Average diurnal variation of SO_2 and CO during LD2020 and LD2021 and coinciding base year 2019. Continuous line and the dotted line represent the mean and median respectively at site#1 and site#2. (c) Average diurnal variation of NO_2, NO_x and O_3 during LD2020 and LD2021 and coinciding base year 2019. Continuous line and the dotted line represent the mean and median respectively at site #1 and site #2.

Author Contributions: A.C.: methodology, formal analysis, data curation, writing—original draft, and writing—review and editing; P.K. (Pradeep Kumar): formal analysis, data curation and writing—review and editing; S.K.S. (Saroj Kumar Sahu): review and editing; C.P.: review and editing; P.K.J.: review and editing; S.K.S. (Sudhir Kumar Singh): review and editing; P.K. (Pankaj Kumar): review and editing; C.A.M.: review and editing; A.K.S.: review and editing; B.T.: review and editing. All authors have read and agreed to the published version of the manuscript.

Funding: A.C. acknowledges the Rashtriya Uchchatar Shiksha Abhiyan (RUSA) Post-Doctoral Fellowship (PDF) scheme, order no. RUSA-1041-2016(PDF-XVIII) 25986/2020, for the financial support under RUSA 2.0 project. P.K. acknowledges UGC, for the DS Kothari PDF awarded via UGC sanction No.F.4-2/2006 (BSR)/ES/18-19/0041.

Institutional Review Board Statement: Not applicable.

Informed Consent Statement: Not applicable.

Data Availability Statement: There are no associated data with this manuscript. Raw data will be made available as per request.

Acknowledgments: The authors are thankful for the NASA POWER website and CPCB, Govt. of India for providing the access to the datasets. Author Sudhir Kumar Singh thanks to Coordinator and DST-FIST for providing infrastructural facilities to KBCASO, University of Allahabad.

Conflicts of Interest: The authors declare no conflict of interest.

References

1. Li, X.; Jin, L.; Kan, H. *Air Pollution: A Global Problem Needs Local Fixes*; Springer Nature: Cham, Switzerland, 2019; pp. 437–439.
2. Caselles, J.; Colliga, C.; Zornoza, P. Evaluation of trace element pollution from vehicle emissions in petunia plants. *Water Air Soil Pollut.* **2002**, *136*, 1–9. [CrossRef]
3. Curtis, L.; William, R.; Patricia, S.W.; Ervin, F.; Yaqin, P. Adverse health effects of outdoor air pollutants. *Environ. Int.* **2006**, *32*, 815–830. [CrossRef]
4. World Health Organization. *Air Pollution and Child Health: Prescribing Clean Air: Summary (No. WHO/CED/PHE/18.01)*; World Health Organization: Geneva, Switzerland, 2018.
5. Kumar, P.; Pratap, V.; Kumar, A.; Choudhary, A.; Prasad, R.; Shukla, A.; Singh, R.P.; Singh, A.K. Assessment of atmospheric aerosols over Varanasi: Physical, optical and chemical properties and meteorological implications. *J. Atmos. Sol. Terr. Phys.* **2020**, *209*, 105424. [CrossRef]
6. Kumar, P.; Kapur, S.; Choudhary, A.; Singh, A.K. Spatiotemporal variability of optical properties of aerosols over the Indo-Gangetic Plain during 2011–2015. *Indian J. Phys.* **2022**, *96*, 329–341. [CrossRef]
7. Gurjar, B.R.; Ravindra, K.; Nagpure, A.S. Air pollution trends over Indian megacities and their local-to-global implications. *Atmos. Environ.* **2016**, *142*, 475–495. [CrossRef]
8. Choudhary, A.; Gokhale, S. Urban real-world driving traffic emissions during interruption and congestion. *Transp. Res. D Trans. Environ.* **2016**, *43*, 59–70. [CrossRef]
9. Schembari, C.; Cavalli, F.; Cuccia, E.; Hjorth, J.; Calzolai, G.; Pérez, N.; Pey, J.; Prati, P.; Raes, F. Impact of a European directive on ship emissions on air quality in Mediterranean harbours. *Atmos. Environ.* **2012**, *61*, 661–669. [CrossRef]
10. Choudhary, A.; Gokhale, S. Evaluation of emission reduction benefits of traffic flow management and technology upgrade in a congested urban traffic corridor. *Clean Technol. Environ. Pol.* **2019**, *21*, 257–273. [CrossRef]
11. Shah, K.; Amin, N.; Ahmad, I.; Shah, S.; Hussain, K. Dust particles induce stress, reduce various photosynthetic pigments and their derivatives in Ficus benjamina: A landscape plant. *Int. J. Agric. Biol.* **2017**, *19*, 1469–1474.
12. Strak, M.; Janssen, N.A.; Gosens, I.; Cassee, F.R.; Lebret, E.; Godri, K.J.; Mudway, I.S.; Kelly, F.J.; Harrison, R.M.; Brunekreef, B.; et al. Airborne particulate matter and acute lung inflammation: Strak et al. respond. *Environ. Health Perspect.* **2013**, *121*, a11–a12. [CrossRef]
13. Atkinson, R.W.; Cohen, A.; Mehta, S.; Anderson, H.R. Systematic review and meta-analysis of epidemiological time-series studies on outdoor air pollution and health in Asia. *Air Qual. Atmos. Health* **2012**, *5*, 383–391. [CrossRef]
14. Wong, C.M.; Vichit-Vadakan, N.; Kan, H.; Qian, Z. Public Health and Air Pollution in Asia (PAPA): A multicity study of short-term effects of air pollution on mortality. *Environ. Health Perspect.* **2008**, *116*, 1195–1202. [CrossRef]
15. Shang, Y.; Sun, Z.; Cao, J.; Wang, X.; Zhong, L.; Bi, X.; Li, H.; Liu, W.; Zhu, T.; Huang, W. Systematic review of Chinese studies of short-term exposure to air pollution and daily mortality. *Environ Int.* **2013**, *54*, 100–111. [CrossRef]
16. Venter, Z.S.; Aunan, K.; Chowdhury, S.; Lelieveld, J. COVID-19 lockdowns cause global air pollution declines. *Proc. Natl. Acad. Sci. USA* **2020**, *117*, 18984–18990. [CrossRef]
17. Saadat, S.; Rawtani, D.; Hussain, C.M. Environmental perspective of COVID-19. *Sci. Total Environ.* **2020**, *728*, 138870. [CrossRef]
18. Sharma, S.; Zhang, M.; Gao, J.; Zhang, H.; Kota, S.H. Effect of restricted emissions during COVID-19 on air quality in India. *Sci. Total Environ.* **2020**, *728*, 138878. [CrossRef] [PubMed]
19. Kumar, P.; Hama, S.; Omidvarborna, H.; Sharma, A.; Sahani, J.; Abhijith, K.V.; Debele, S.E.; Zavala-Reyes, J.C.; Barwise, Y.; Tiwari, A. Temporary reduction in fine particulate matter due to 'anthropogenic emissions switch-off' during COVID-19 lockdown in Indian cities. *Sustain. Cities Soc.* **2020**, *62*, 102382. [CrossRef] [PubMed]
20. Das, L.; Patri, M. Impact of Environmental Pollution on Respiratory System of Human and Animals in Angul and Talcher Industrial Areas, Odisha, India: A Case Study. *Int. J. Zoo. Animal Biol.* **2019**, *2*, 000162.
21. Hota, P.; Behera, B. Coal mining in Odisha: An analysis of impacts on agricultural production and human health. *Extr. Ind. Soc.* **2015**, *2*, 683–693. [CrossRef]
22. Cropper, M.; Gamkhar, S.; Malik, K.; Limonov, A.; Partridge, I. The health effects of coal electricity generation in India. *Resour. Future Discuss. Pap.* **2012**, 12–25. [CrossRef]
23. Mishra, N.; Das, N. Coal Mining and Local Environment: A Study in Talcher Coalfield of India. *Air Soil Water Res.* **2017**, *10*, 1–17. [CrossRef]

24. MSME. *Brief Industrial Profile of Angul District*; MSME: New Delhi, India, 2020.
25. Annual Report, 2021a. Annual Ruteen Environmental Monitoring Report 2019–2020, Talcher Coalfield. Available online: https://www.mahanadicoal.in/Environment/Environmental_Monitoring_Report.php (accessed on 15 June 2022).
26. Annual Report, 2021b. Annual Ruteen Environmental Monitoring Report 2019–2020, IB-Valley Coalfield. Available online: https://www.mahanadicoal.in/Environment/Environmental_Monitoring_Report.php (accessed on 15 June 2022).
27. CPCB. *Air Quality Comparison Report*; Central Pollution Control Board: New Delhi, India, 2020.
28. Hu, J.; Ying, Q.; Wang, Y.; Zhang, H. Characterizing multi-pollutant air pollution in China: Comparison of three air quality indices. *Environ. Int.* **2015**, *84*, 17–25. [CrossRef] [PubMed]
29. Ghude, S.D.; Chate, D.M.; Jena, C.; Beig, G.; Kumar, R.; Barth, M.C.; Pfister, G.G.; Fadnavis, S.; Pithani, P. Premature mortality in India due to $PM_{2.5}$ and ozone exposure. *Geophys. Res. Lett.* **2016**, *43*, 4650–4658. [CrossRef]
30. Shanmugam, K. The value of life: Estimates from Indian Labour Market. *Indian Econ. J.* **1996**, *44*, 105–114. [CrossRef]
31. Cropper, M.; Simon, N.B.; Alberini, A.; Arora, S. *Valuing Mortality Reductions in India: A Study of Compensating-Wage Differentials*; World Bank Group: Washington, DC, USA, 1999. [CrossRef]
32. Bherwani, H.; Nair, M.; Musugu, K.; Gautam, S.; Gupta, A.; Kapley, A.; Kumar, R. Valuation of air pollution externalities: Comparative assessment of economic damage and emission reduction under COVID-19 lockdown. *Air Qual. Atmos. Health* **2020**, *13*, 683–694. [CrossRef] [PubMed]
33. Sathe, Y.; Gupta, P.; Bawase, M.; Lamsal, L.; Patadia, F.; Thipse, S. Surface and satellite observations of air pollution in India during COVID-19 lockdown: Implication to air quality. *Sustain. Cities Soc.* **2021**, *66*, 102688. [CrossRef] [PubMed]
34. Parida, B.R.; Bar, S.; Roberts, G.; Mandal, S.P.; Pandey, A.C.; Kumar, M.; Dash, J. Improvement in air quality and its impact on land surface temperature in major urban areas across India during the first lockdown of the pandemic. *Environ. Res.* **2021**, *199*, 111280. [CrossRef]
35. Thomas, J.; Jainet, P.J.; Sudheer, K.P. Ambient air quality of a less industrialized region of India (Kerala) during the COVID-19 lockdown. *Anthropocene* **2020**, *32*, 100270. [CrossRef]
36. Resmi, C.T.; Nishanth, T.; Satheesh Kumar, M.K.; Manoj, M.G.; Balachandramohan, M.; Valsaraj, K.T. Air quality improvement during triple-lockdown in the coastal city of Kannur, Kerala to combat COVID-19 transmission. *Peer J.* **2020**, *8*, e9642. [CrossRef]
37. Sahu, S.K.; Beig, G.; Parkhi, N. Critical emissions from the largest on-road transport network in South Asia. *Aerosol Air Qual. Res.* **2014**, *14*, 135–144. [CrossRef]
38. Singh, V.; Biswal, A.; Kesarkar, A.P.; Mor, S.; Ravindra, K. High resolution vehicular PM_{10} emissions over megacity Delhi: Relative contributions of exhaust and non-exhaust sources. *Sci. Total Environ.* **2020**, *699*, 134273. [CrossRef] [PubMed]
39. Lu, Z.; Streets, D.G. Increase in NO_x emissions from Indian thermal power plants during 1996–2010: Unit-based inventories and multi satellite observations. *Environ. Sci. Technol.* **2012**, *46*, 7463–7470. [CrossRef] [PubMed]
40. Ghude, S.D.; Fadnavis, S.; Beig, G.; Polade, S.D.; Van Der A, R.J. Detection of surface emission hot spots, trends, and seasonal cycle from satellite-retrieved NO_2 over India. *J. Geophys. Res. Atmos.* **2008**, *113*, D20. [CrossRef]
41. Garg, A.; Shukla, P.R.; Bhattacharya, S.; Dadhwal, V.K. Sub-region (district) and sector level SO_2 and NO_x emissions for India: Assessment of inventories and mitigation flexibility. *Atmos. Environ.* **2001**, *35*, 703–713. [CrossRef]
42. Mahato, S.; Ghosh, K.G. Short-term exposure to ambient air quality of the most polluted Indian cities due to lockdown amid SARS-CoV-2. *Environ. Res.* **2020**, *188*, 109835. [CrossRef]
43. Mallik, C.; Mahapatra, P.S.; Kumar, P.; Panda, S.; Boopathy, R.; Das, T.; Lal, S. Influence of regional emissions on SO_2 concentrations over Bhubaneswar, a capital city in eastern India downwind of the Indian SO_2 hotspots. *Atmos. Environ.* **2019**, *209*, 220–232. [CrossRef]
44. Hendryx, M.; Zullig, K.J.; Luo, J. Impacts of coal use on health. *Annu. Rev. Public Health* **2020**, *41*, 397–415. [CrossRef] [PubMed]
45. Mishra, S.K. Putting value to human health in coal mining region of India. *J. Health Manag.* **2015**, *17*, 339–355. [CrossRef]
46. Guttikunda, S.K.; Jawahar, P. Evaluation of particulate pollution and health impacts from planned expansion of coal-fired thermal power plants in India using WRF-CAMx modeling system. *Aerosol Air Qual. Res.* **2018**, *18*, 3187–3202. [CrossRef]
47. Cropper, M.; Cui, R.; Guttikunda, S.; Hultman, N.; Jawahar, P.; Park, Y.; Yao, X.; Song, X.P. The mortality impacts of current and planned coal-fired power plants in India. *Proc. Natl. Acad. Sci. USA* **2021**, *118*, e2017936118. [CrossRef]
48. Lal, S.; Naja, M.; Subbaraya, B.H. Seasonal variations in surface ozone and its precursors over an urban site in India. *Atmos. Environ.* **2000**, *34*, 2713–2724. [CrossRef]
49. Reddy, B.S.; Kumar, K.R.; Balakrishnaiah, G.; Gopal, K.R.; Reddy, R.R.; Sivakumar, V.; Lingaswamy, A.P.; Arafath, S.M.; Umadevi, K.; Kumari, S.P.; et al. Analysis of diurnal and seasonal behavior of surface ozone and its precursors (NO_x) at a semi-arid rural site in southern India. *Aerosol Air Qual. Res.* **2012**, *12*, 1081–1094. [CrossRef]
50. Kumar, V.; Sinha, V. Season-wise analyses of VOCs, hydroxyl radicals and ozone formation chemistry over north-west India reveal isoprene and acetaldehyde as the most potent ozone precursors throughout the year. *Chemosphere* **2021**, *283*, 131184. [CrossRef] [PubMed]
51. Ampah, J.D.; Jin, C.; Agyekum, E.B.; Afrane, S.; Geng, Z.; Adun, H.; Yusuf, A.A.; Liu, H.; Bamisile, O. Performance analysis and socio-enviro-economic feasibility study of a new hybrid energy system-based decarbonization approach for coal mine sites. *Sci. Total Environ.* **2022**, *854*, 158820. [CrossRef] [PubMed]